Journal of Southeast University (English Edition) Vol. 23, No. 1, pp. 7 – 11 Mar. 2007 ISSN 1003—7985

Low complexity iterative differential decoding algorithm for multiband UWB communication systems

Jin Xiufeng Bi Guangguo Xiao Haiyong

(National Mobile Communications Research Laboratory, Southeast University, Nanjing 210096, China)

Abstract: Due to not requiring channel state information (CSI) at both the transmitter and the receiver, noncoherent ultra-wideband (UWB) incurs a performance penalty of approximately 3 dB in the required signal to noise ratio (SNR) compared to the coherent case. To overcome the gap, an effective differential encoding and decoding scheme for multiband UWB systems is proposed. The proposed scheme employs the parallel concatenation of two recursive differential unitary space-frequency encoders at the transmitter. At the receiver, two component decoders iteratively decode information bits by interchanging soft metric values between each other. To reduce the computation complexity, a decoding algorithm which only uses transition probability to calculate the log likelihood ratios (LLRs) for the decoded bits is given. Simulation results show that the proposed scheme can dramatically outperform the conventional differential and even coherent detection at high SNR with a few iterations.

Key words: multiband UWB; multiple-input multiple-output (MIMO) system; noncoherent detection; group code; iterative decoding

Ultra-wideband (UWB) is a fast emerging technology that offers great potential for the design of high-rate, low-power and short-range wireless indoor and ad hoc networks. According to the Federal Communications Commission's (FCC) UWB definition, UWB transmission is any wireless transmission scheme that occupies a bandwidth of more than 20% of its center frequency or more than 500 MHz. Depending on how the available bandwidth is utilized, UWB systems can be divided into two groups: single band and multiband. In single band UWB systems, the information is directly modulated into a sequence of impulse-like waveforms, which occupy the entire available bandwidth of 7.5 GHz[1]. For multiband UWB systems, the whole bandwidth is divided into several subbands. Each subband occupies a bandwidth of at least 500 MHz in compliance with the FCC regulations. To efficiently capture the multipath energy, orthogonal frequency division multiplexing (OFDM) technique has been used to modulate the information in each subband[2].

Multiple-input multiple-output (MIMO) is a multiple antenna technique that can greatly increase the channel capacity and system performance[3-4]. Most UWB applications are in rich scattering indoor environments, which provide an ideal transmission scenario for MIMO implementation. In addition, as UWB uses microwave frequencies in the 3.1 to 10.6 GHz range, the antenna element separation required for signal orthogonality is small. Consequently, a multiple-antenna UWB communication system is a leading candidate that can meet the very high data rate requirements for future short range wireless communications.

Up to now, most research work on MIMO UWB has adopted a common assumption that channel state information (CSI) is perfectly known at the receiver[5]. This is not a reasonable assumption in practice. Acquiring knowledge of the fading coefficients in a MIMO channel has already been very challenging in the frequency-flat fading case. For multiple-antenna UWB systems, the bandwidth is much greater than the channel coherence bandwidth, inducing severe frequency-selectivity to the system. In this case, obtaining the fading coefficients becomes more difficult due to the presence of multiple paths, which results in an increased number of parameters to be estimated. Hence, it is desirable to develop techniques that do not require channel estimation at the receiver.

Differential space-time modulation for multiple-antenna schemes was proposed in Refs. [6 – 7], illustrating how temporal and spatial diversity can be simultaneously exploited without knowledge of perfect CSI. Although the fading gain is not required at re-

Received 2006-08-31.

Foundation item: The Higher Education Technology Foundation of Huawei Technologies Co., Ltd. (No. YJCB2005016WL).

Biographies: Jin Xiufeng (1977—), male, graduate; Bi Guangguo (corresponding author), male, professor, bigg@seu.edu.cn.

ceivers, the performance loss is about 3 dB in very slow fading, compared to that of the coherent detection case where the fading gain is known. When the fading changes rapidly, the performance loss is significant. More recently, a differential encoding and decoding scheme for multiband UWB systems was proposed in Ref. [8]. By a technique of band hopping in combination with jointly coding across spatial, temporal and frequency domains, the scheme is able to explore the available spatial and multipath diversities.

Motivated by turbo principle in Ref. [9], in this paper, we develop a differential encoding and decoding scheme for multiband MIMO UWB systems. In the proposed scheme, the information is encoded by two differential unitary space-frequency encoders which are parallel concatenated by a symbol interleaver. The receiver consists of two soft decision decoders which exchange extrinsic information iteratively. Due to differentially encoding/decoding in the frequency domain, the proposed scheme does not depend on the assumption that the fading channel stays constant within several OFDM symbol durations. This also reduces the decoding delay.

1 System and Channel Model

Consider a point-to-point multi-band UWB system equipped with M_T transmit antennas and M_R receive antennas as shown in Fig. 1. Within each subband, OFDM modulation with N subcarriers is used at each transmit antenna. At the k-th OFDM block, the channel pulse response from the i-th transmit antenna to the j-th receive antenna can be expressed as[10]

$$h_{ij}^k(t) = \sum_{c=0}^{C}\sum_{l=0}^{L}\alpha_{ij}^k(c,l)\delta(t - T_c - \tau_{c,l}) \quad (1)$$

where $i = 1, 2, \ldots, M_T$ and $j = 1, 2, \ldots, M_R$. The value $\alpha_{ij}^k(c, l)$ denotes the channel coefficient of the l-th multipath component in the c-th cluster at time k from the i-th transmit antenna to the j-th receive antenna. The time duration T_c denotes the arrival time of the c-th cluster, and $\tau_{c,l}$ is the delay of the l-th multipati component in the c-th cluster relative to the cluster arrival time T_c. The cluster arrivals and the ray arrivals within each cluster can be modeled as Poisson distribution with rate Λ and λ (where $\lambda > \Lambda$), respectively. The amplitude of the channel coefficient $|\alpha_{ij}^k(c, l)|$ can follow the log-normal distribution, the Nakagami distribution, or the Rayleigh distribution while the phase $\angle\alpha_{ij}^k(c, l)$ is uniformly distributed over $[0, 2\pi)$. According to the channel standard[10], the log-normal distribution seems to better fit the measurement data. So it is chosen for the amplitude of the channel coefficient $|\alpha_{ij}^k(c, l)|$ in this paper.

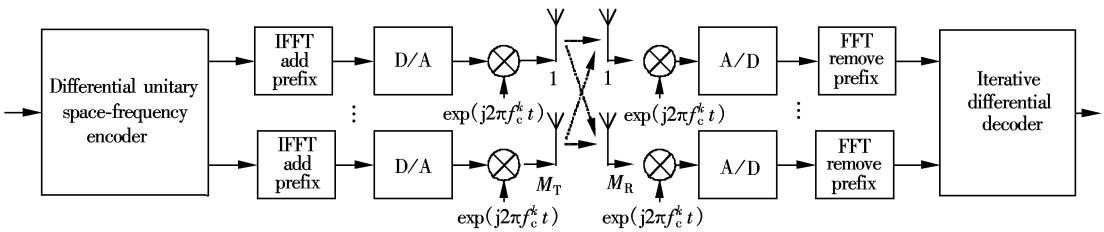

Fig. 1 Multiband-OFDM MIMO UWB system

Let $x_i^k(n)$ denote the data symbol transmitted from the i-th transmit antenna at the n-th subcarrier during the k-th OFDM symbol period. At the receiver, after cyclic prefix removing and OFDM demodulating, the received signal at the n-th subcarrier at receive antenna j during the k-th OFDM symbol duration can be expressed as

$$y_j^k(n) = \sqrt{\frac{E}{M_T}}\sum_{i=1}^{M_T} x_i^k(n)H_{ij}^k(n) + \omega_j^k(n) \quad (2)$$

The factor $\sqrt{E/M_T}$ guarantees that the average energy per transmitted symbol is E, independent of the number of transmit antennas, and

$$H_{ij}^k(n) = \sum_{c=0}^{C}\sum_{l=0}^{L}\alpha_{ij}^k(c,l)\exp[-j2\pi n\Delta f(T_c + \tau_{c,l})] \quad (3)$$

where Δf is the frequency separation between two adjacent subcarriers. The noise sample at the n-th subcarrier is modeled as a complex Gaussian random variable with zero mean and a two-sided power spectral density of $N_0/2$.

2 Differential Encoding Scheme

In this section, we describe the differential encoding scheme at the transmitter. The block diagram of the encoder is presented in Fig. 2. Two differential unitary space-frequency encoders are connected in parallel concatenation, separated by a symbol interleaver. Information bits are directly fed into encoder 1 and after interleaving, fed into encoder 2. The outputs of the two component encoders are transmitted alter-

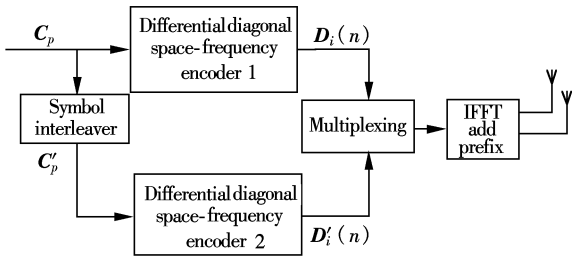

Fig. 2 Differential encoding system

nately in two OFDM symbol periods.

Differential unitary space-time block code was proposed in Ref. [6] based on unitary group codes. In this paper, we perform the group differential encoding in frequency domain instead of encoding in time domain. For our encoding scheme, we only consider two transmit antennas at the transmitter. The constellation is BPSK. Then the BPSK group $\boldsymbol{G}$ has four 2×2 unitary matrices[6]:

$$\boldsymbol{G} = \left\{ \pm \begin{bmatrix} 1 & 0 \\ 0 & 1 \end{bmatrix}, \pm \begin{bmatrix} 0 & 1 \\ -1 & 0 \end{bmatrix} \right\}$$

Dividing the information bits into vectors $\boldsymbol{C}_p = \{c_{p,1}, c_{p,2}, \ldots, c_{p,N-2}\}$, where p denotes the time index. Giving two input bits $c_{p,2n-1}$, $c_{p,2n}$ ($n = 1, 2, \ldots, N/2-1$) the encoder chooses a unitary matrix $\boldsymbol{G}_n$ according to the mapping rule:

$$00: \boldsymbol{G}_0 \rightarrow \begin{bmatrix} +1 & 0 \\ 0 & +1 \end{bmatrix} \quad 10: \boldsymbol{G}_2 \rightarrow \begin{bmatrix} -1 & 0 \\ 0 & -1 \end{bmatrix}$$

$$01: \boldsymbol{G}_1 \rightarrow \begin{bmatrix} +i & 0 \\ 0 & +i \end{bmatrix} \quad 01: \boldsymbol{G}_3 \rightarrow \begin{bmatrix} -i & 0 \\ 0 & -i \end{bmatrix}$$

The differential transmission equation for encoder 1 can be expressed as

$$\begin{bmatrix} D_1(2n+1) & D_1(2n+2) \\ D_2(2n+1) & D_2(2n+2) \end{bmatrix} = \begin{bmatrix} D_1(2n-1) & D_1(2n) \\ D_2(2n-1) & D_2(2n) \end{bmatrix} \boldsymbol{G}_n \tag{4}$$

where $D_i(n)$ denotes the symbol transmitted at the n-th subcarrier from the i-th transmitter. The differential transmission is initiated by sending a reference matrix $\boldsymbol{D}_0$ at the first two subcarriers during each OFDM symbol period.

$$\boldsymbol{D}_0 = \begin{bmatrix} D_1(1) & D_1(2) \\ D_2(1) & D_2(2) \end{bmatrix} = \begin{bmatrix} 1 & -1 \\ 1 & 1 \end{bmatrix} \tag{5}$$

The encoding process for encoder 2 is the same as encoder 1 except that the input data are different. From Eq. (4), it can be seen that the differential space-frequency encoder has a recursive structure similar to DPSK or recursive convolutional codes. So the encoder can be described by the trellis shown in Fig. 3.

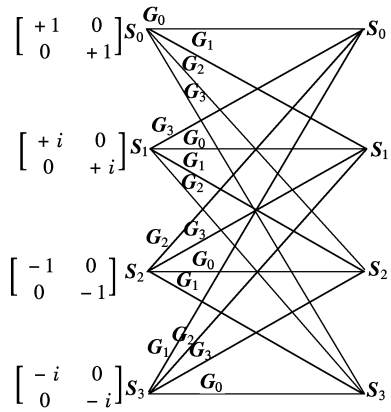

Fig. 3 Trellis structure of differential group codes

3 Iterative Decoding Scheme

The block diagram of the iterative decoder is depicted in Fig. 4. At the receiver, the demodulated symbols $\boldsymbol{Y}_p^1$ and $\boldsymbol{Y}_p^2$ are first fed into component decoder 1 and component decoder 2, respectively. In addition, each component decoder also takes *a priori* information from the other component decoder about the likely values of the bit concerned. Employing the two sets of values, each component decoder uses a soft input soft output decoding algorithm to compute the log likelihood ratios (LLRs) for the decoded bits.

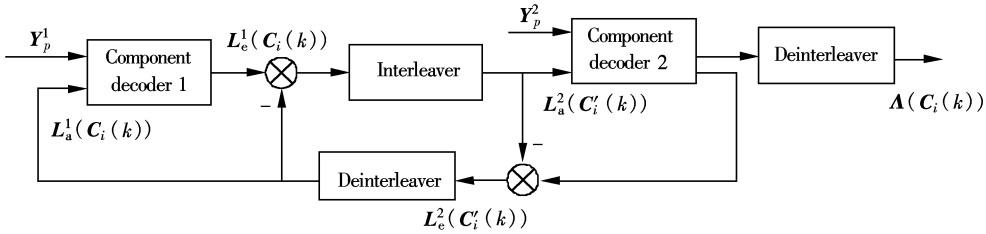

Fig. 4 Block diagram of the iterative decoder

To obtain the soft output values of the information bits, the BCJR algorithm[11] can be used in each component decoder. However, the BCJR algorithm not only has considerable computational complexity in itself, but also does not function properly in decoding the differential group codes because of the special structure of the trellis that each state has the same number of branches as the total number of states. Hence, we adopt a low complexity scheme which only uses the transition probability $\gamma_{s',s}$ to calculate the

LLRs for the decoded bits.

Considering component decoder 1, we first divide the information bits vector $\boldsymbol{c}_p$ into sub-blocks as follows:

$$\boldsymbol{C} = \boldsymbol{c}_p = \{c_{p,1}, c_{p,2}, \ldots, c_{p,N-2}\} = \{\boldsymbol{C}_1, \boldsymbol{C}_2, \ldots, \boldsymbol{C}_{\frac{N}{2}-1}\} \tag{6}$$

Each sub-block contains two adjacent information bits. Correspondingly, the partition of the encoder output $\boldsymbol{D}_i$ and receive symbol $\boldsymbol{Y}_p^1$ can be expressed as

$$\begin{aligned} \boldsymbol{D} &= \boldsymbol{D}_i = \{\boldsymbol{D}^1, \boldsymbol{D}^2, \ldots, \boldsymbol{D}^{\frac{N}{2}}\} \\ \boldsymbol{Y} &= \boldsymbol{Y}_p^1 = \{\boldsymbol{Y}_1, \boldsymbol{Y}_2, \ldots, \boldsymbol{Y}_{\frac{N}{2}}\} \end{aligned} \tag{7}$$

where $\boldsymbol{D}^k$ is a 2×2 unitary matrix and $\boldsymbol{D}^1 = \boldsymbol{D}_0 = \begin{bmatrix} 1 & -1 \\ 1 & 1 \end{bmatrix}$ is the reference signal matrix.

In the absence of CSI, when $\boldsymbol{D}^k$ is transmitted, the conditional probability of the receive signal $\boldsymbol{Y}_k$ is[6]

$$p(\boldsymbol{Y}_k \mid \boldsymbol{D}^k) \propto \exp\left\{\frac{1}{2(\sigma^2+1)}(\mathrm{ReTr}\{\boldsymbol{G}_k \boldsymbol{Y}_k^{\dagger} \boldsymbol{Y}_{k-1}\})\right\} \tag{8}$$

Then, in our decoding scheme, the LLRs of the information bits $\boldsymbol{C}_k = [c_{p,2k-1}, c_{p,2k}] = [C_k(1), C_k(2)]$ can be calculated as

$$\begin{aligned} \Lambda(C_k(i)) &= \ln \frac{\sum_{(s',s) \in A_{C_k(i)=1}} \gamma_k(s', s)}{\sum_{(s',s) \in A_{C_k(i)=0}} \gamma_k(s', s)} = \\ &\ln \frac{\sum_{(s',s) \in A_{C_k(i)=1}} p(\boldsymbol{Y}_k \mid \boldsymbol{D}^k) p(\boldsymbol{G}_k)}{\sum_{(s',s) \in A_{C_k(i)=0}} p(\boldsymbol{Y}_k \mid \boldsymbol{D}^k) p(\boldsymbol{G}_k)} = \\ &\ln \frac{\sum_{(s',s) \in A_{C_k(i)=1}} p(\boldsymbol{Y}_k \mid \boldsymbol{D}^k) \left(\prod_{i=1}^{2} p(C_k(i) = q) \right)}{\sum_{(s',s) \in A_{C_k(i)=0}} p(\boldsymbol{Y}_k \mid \boldsymbol{D}^k) \left(\prod_{i=1}^{2} p(C_k(i) = q) \right)} \end{aligned} \tag{9}$$

where $p(C_k(i) = q)$ is the *a priori* probability of bit $C_k(i)$. It can be obtained using the following equation:

$$p(C_k(i) = q) = \begin{cases} \dfrac{1}{1 + \exp\{L_a(C_k(i))\}} & q = 0 \\ \dfrac{\exp\{L_a(C_k(i))\}}{1 + \exp\{L_a(C_k(i))\}} & q = 1 \end{cases} \tag{10}$$

During the first iteration, the *a priori* information, $L_a(C_k(i))$, for component decoder 1, is taken as zero. After the final iteration, the decision of the information bits are made such that

$$\hat{C}_k(i) = \begin{cases} 1 & \Lambda(C_k(i)) \geqslant 0 \\ 0 & \Lambda(C_k(i)) < 0 \end{cases} \tag{11}$$

4 Simulation Results

We performed simulations for multiband MIMO UWB systems with $N = 512$ subcarriers and the subband bandwidth $W = 500$ MHz. Two transmit antennas and one receive antenna are used. The channel model parameters followed those for CM1 and CM2[10]. The differential encoded OFDM symbols are transmitted alternately in two consecutive symbol periods.

Fig. 5 depicts the performance of the iterative differential decoding scheme under CM1. For clarity, only the results with one and three iterations are shown. We also give the performance of conventional differential detection and coherent detection. For comparing performance under the same spectral efficiency, each OFDM symbol is repeatedly transmitted in two consecutive OFDM symbol periods for conventional differential detection and coherent detection. It can be seen that, at low SNR, the iterative decoding scheme has a poor performance compared to the coherent detection, but still outperforms the conventional differential detection. At the BER of 10^{-3}, the proposed scheme yields 5 dB improvement over conventional differential detection. With the increase of the SNR, the iterative scheme even outperforms the coherent detection. At the BER of 10^{-4}, the performance gain is nearly 3 dB against coherent detection.

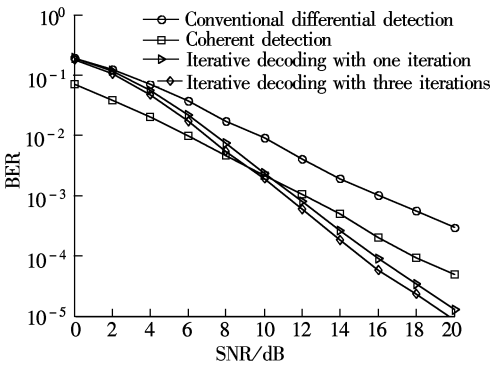

Fig. 5 Performance of the iterative differential decoding scheme under CM1

Fig. 6 presents the performance of three schemes under CM2. The performance improved by the proposed scheme is also significant. At the BER of 10^{-3}, the performance gain is 6 dB relative to conventional differential detection. Compared with coherent detection, the performance gain is 3 dB at the BER of 10^{-4}.

In both Fig. 5 and Fig. 6, we also give the performance of the iterative decoding scheme after the first iteration. It is shown that most of the performance

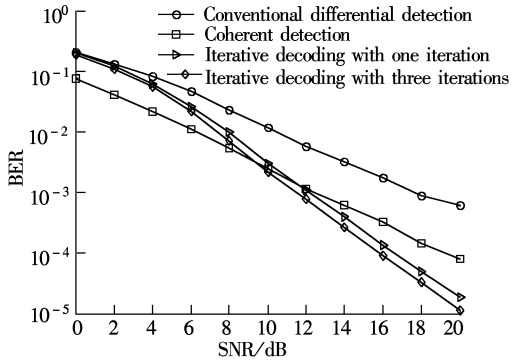

Fig. 6 Performance of the iterative differential decoding scheme under CM2

gain can be achieved during the first iteration under both CM1 and CM2.

5 Conclusion

In this paper, an iterative differential decoding scheme for multiband OFDM MIMO systems is presented. The decoding delay system comprises two parallel concatenated differential encoders. Due to differential decoding delay in frequency domain, the decoding delay is much smaller than the differential decoding delay in time domain. A low complexity soft decision decoding algorithm is given to calculate the LLRs of the decoded bits. Simulation results demonstrate that the presented scheme yields superior performance to the conventional differential detection and even outperforms coherent detection at high SNR. At the BER of 10^{-4}, the performance gain is up to 3 dB against uncoded coherent detection under CM1 and CM2. It is also expected that the system performance can be further improved by using more receive antennas.

References

[1] Win Moe Z, Scholtz Robert A. Impulse radio: How it works [J]. *IEEE Communications Letters*, 1998, **2**(2): 36 – 38.

[2] Batra Anuj, Balakrishnan Jaiganesh, Aiello G Roberto, et al. Design of a multiband OFDM system for realistic UWB channel environments [J]. *IEEE Transactions on Microwave Theory and Techniques*, 2004, **52**(9): 2123 – 2138.

[3] Foschini G J, Gans M J. On limits of wireless communications in a fading environment when using multiple antennas[J]. *Wireless Personal Communications*, 1998, **6**(3): 311 – 335.

[4] Tarokh V, Seshadri N, Calderbank A. Space-time codes for high data rate wireless communications: performance criterion and code construction[J]. *IEEE Transactions on Information Theory*, 1998, **44**(3): 744 – 765.

[5] Siriwongpairat W P, Su W, Olfat M, et al. Space-time-frequency coded multiband UWB communication systems [J]. *IEEE Wireless Communications and Networking Conference*, 2005, **1**(3): 426 – 431.

[6] Hughes B L. Differential space-time modulation [J]. *IEEE Transactions on Information Theory*, 2000, **46**(11): 2567 – 2578.

[7] Hochwald B, Sweldens W. Differential unitary space-time modulation [J]. *IEEE Transactions on Communications*, 2000, **48**(12): 2041 – 2052.

[8] Himsoon T, Su W, Liu K J R. Multiband differential modulation for UWB communication systems [C]//*IEEE Global Telecommunications Conference*. St. Louis, MO, USA, 2005: 3789 – 3793.

[9] Berrou C, Glavieux A. Near optimum error correcting coding and decoding: Turbo-codes[J]. *IEEE Transactions on Communications*, 1996, **44**(10): 1261 – 1271.

[10] Foerster J R. IEEE 802.15-02/490 Channel modeling sub-committee report final[S]. 2003.

[11] Bahl L R, Cocke J, Jelinek F, et al. Optimal decoding of linear codes for minimizing symbol error rate [J]. *IEEE Transactions on Information Theory*, 1974, **20**(3): 284 – 287.

多频带 UWB 通信系统中低复杂度迭代差分译码算法

金秀峰　毕光国　肖海勇

(东南大学移动通信国家重点实验室,南京 210096)

摘要:相对于相干检测,由于在收发端不需要信道状态信息,非相干 UWB 通信在信噪比方面会有近 3 dB 的性能损失. 为了克服这一性能差距,提出了一种有效的基于多频带 UWB 系统的差分编译码方案. 该方案在发射端使用 2 个并行级联的递归酉差分空频编码器对数据进行编码. 接收端的 2 个分量译码器通过互相交换软度量值对数据进行译码. 为了降低接收机的计算复杂度,给出一种只使用转移概率计算信息比特似然比的译码算法. 仿真结果表明,在较少迭代次数下,算法性能远优于传统非相干检测,在高信噪比时,其性能甚至超过了相干检测.

关键词:多频带 UWB;多输入多输出(MIMO)系统;非相干检测;群码;迭代译码

中图分类号:TN911.2